EUR 2506.e

EUROPEAN ATOMIC ENERGY COMMUNITY - EURATOM

REACTOR POWER REDUCTION IN MINIMUM TIME INCLUDING RESTRICTION OF XENON POISONING

by

W. DE BACKER

1965

Joint Nuclear Research Center
Ispra Establishment - Italy

Scientific Data Processing Center - CETIS

Paper presented at the
Congrès d'Automatique Théorique
Saclay, France - May 4-7, 1965

LEGAL NOTICE

This report can be obtained, at the price of Belgian Francs 40,—
from : PRESSES ACADEMIQUES EUROPEENNES -
98, Chaussée de Charleroi, Brussels 6.

Please remit payments to :

— BANQUE DE LA SOCIETE GENERALE
(Agence Ma Campagne) - Brussels - account No. 964.558,

— BELGIAN AMERICAN BANK AND TRUST COMPANY -
New York - account No. 22.186,

— LLOYDS BANK (Europe) Ltd. - 10 Moorgate - London E.C.2,

giving the reference : «EUR 2506 .e - REACTOR POWER REDUCTION IN MINIMUM TIME INCLUDING RESTRICTION OF XENON POISONING».

Printed by SMEETS, s.a.
Brussels, September 1965.

TABLEAU VII - 1

COEFFICIENTS ISOTHERMES EN pcm/°C

	Coeur	Couverture axiale infér.	Couverture axiale supér.	Couverture radiale	Espace de transition infer.	Espace de transition supér.I	Espace de transition supér.II
Dilatation sodium situé à l'intérieur des gaines hexagonales	+0,340	-0,0032	-0,0015	-0,0302	-0,0326	-0,0603	-0,0135
Dilatation sodium situé entre les gaines hexagonales	+0,054	-0,0007	-0,0003	-0,0065			
Dilatation axiale combustible ou fertile	-0,318	+0,0004	+0,0003	-0,0022		0	
Dilatation axiale gaine aiguille	+0,049	-0,0077	-0,0000	-0,0002		-0,0009	
Dilatation radiale gaine aiguille	+0,040	-0,0007	-0,0004	-0,0066		-0,0075	
Dilatation axiale gaine hexagonale	+0,051	+0,0152	-0,0001	-0,0007		+0,0017	
Dilatation radiale gaine hexagonale	+0,004	-0,0001	-0,0000	-0,0005		-0,0007	
Total	+0,220	+0,003	-0,002	-0,047	-0,033	-0,068	-0,013

TABLEAU VI - 1 (suite)

Coefficients globaux pour le réacteur :

Dilatation sodium	+0,25	
Dilatation axiale combustible (ou fertile)	-0,32	
Dilatation axiale gaine des aiguilles	+0,04	
Dilatation radiale gaine des aiguilles	+0,02	
Dilatation axiale gaine hexagonale	+0,07	
Dilatation radiale gaine hexagonale	+0,00	
	Après compactage	Avant compactage
Effet des plaquettes	-0.70	0
Déformation des assemblages	+0.	-0,
Sommier	-0,13	-0,81
Effet Doppler	-1,15	
Isotherme total	-1,9 pcm/°C	

TABLEAU VII - 2

COEFFICIENTS DE PUISSANCE EN pcm/MW[18)]

	Débit nominal		Débit dixième	
	avant compactage	après compactage	avant compactage	après compactage
Dilatation sodium	+0,0072	+0,0072	+0,072	+0,072
Dilatation axiale combustible	-0,016	-0,016	-0,138	-0,138
Dilatation gaines	+0,0065	+0,0065	+0,057	+0,057
Effet Doppler	-0,40	-0,40	-0,85	-0,85
Effet des plaquettes	0	-0,035	0	-0,035
Coefficient total	-0,40	-0,435	-0,86	-1,21

18)
Pour le réacteur considéré :

$$\beta = 350 \text{ pcm}$$

$$l = 4{,}9 \times 10^{-7} \text{ seconde}$$

Rappelons en outre la définition :

$$1 \text{ pcm} = 10^{-5} \times \delta_{k/k}$$

- au coefficient de puissance pour passer à 2500 MWth : 3,5 $

- à l'usure du combustible (correspondant à un déchargement partiel au bout de 6 mois) : 2 $[14)]

La valeur totale est de 6,9 $.

Or, 7 barres de sécurité/compensation sont prévues, dont la valeur maximale est 2,3 $ environ par barre, ce qui donne une réactivité totale de 16,1 $.

On voit que, compte tenu de la réserve de réactivité nécessaire (6,9$) il reste 9,2 $ pour la sécurité, valeur suffisante pour réduire instantanément la puissance de 90 % en cas d'incident, et pour pallier l'erreur maximale de chargement qui est liée à la capacité des zones d'ajustement recevant les assemblages de types différents. Cette capacité sera inférieure aux 9,2 $ dont on dispose étant donné que les variations de réactivité dues aux tolérances de fabrication sont beaucoup plus faibles. Une tolérance de $\pm$ 1 % sur le poids de PuO2 donne une variation de réactivité de $\pm$ 590 pcm.

III - ETUDE DE LA STABILITE

L'étude de la stabilité du réacteur a été effectuée pour le bloc pile seul en raison du fait que les circuits de refroidissement ne peuvent pas apporter d'instabilité propre. Le code digital utilisé tient compte :

- d'une répartition continue de la température dans la section droite du barreau de combustible
- de la température du sodium, du combustible et de la gaine.

14) Cette estimation est large et comporte une marge importante.

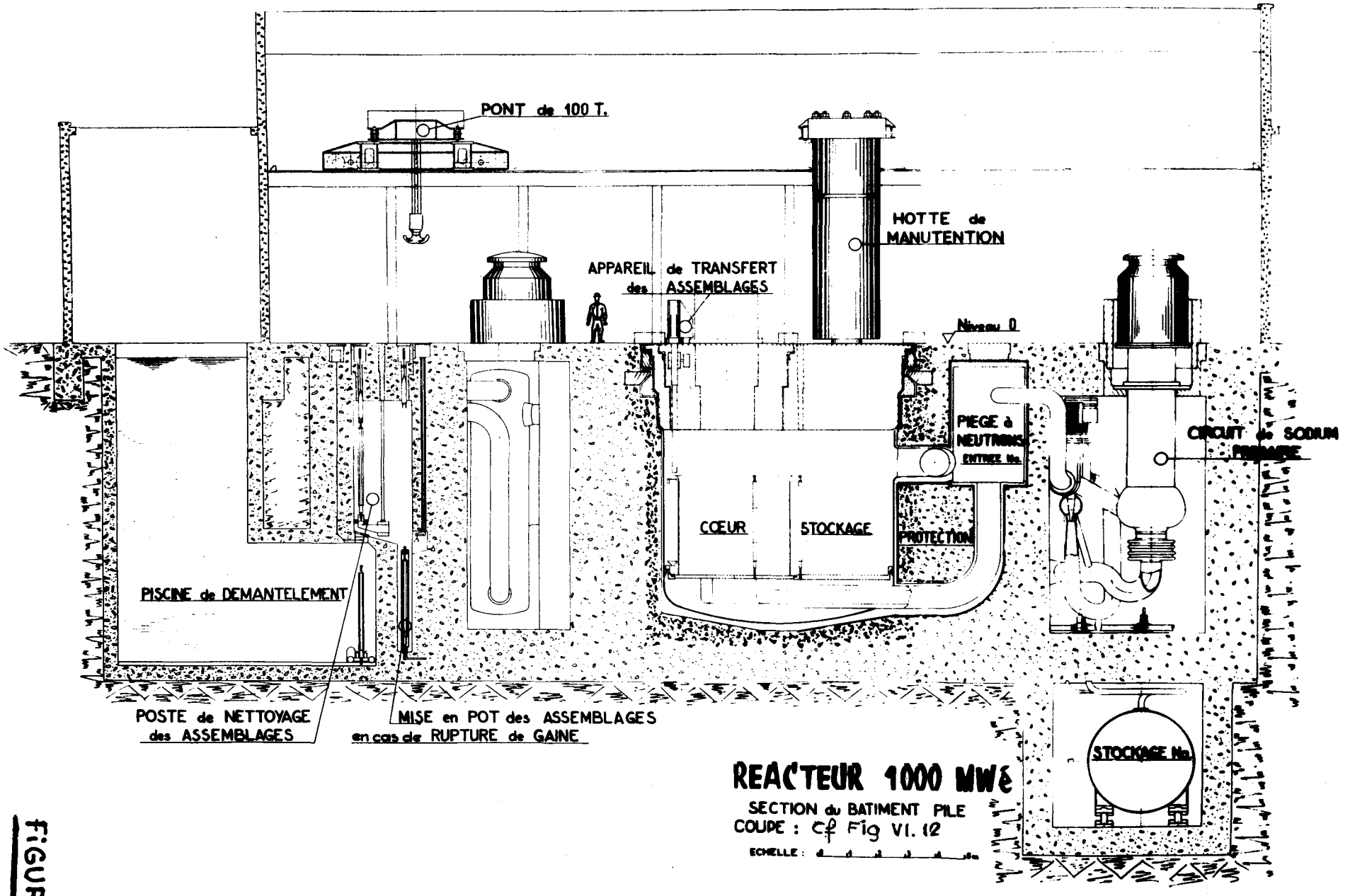
PONT de 100 T.
HOTTE de MANUTENTION
APPAREIL de TRANSFERT des ASSEMBLAGES
Niveau 0
PIEGE à NEUTRONS
ENTREE Na
CIRCUIT de SODIUM PRIMAIRE
CŒUR
STOCKAGE
PROTECTION
PISCINE de DEMANTELEMENT
POSTE de NETTOYAGE des ASSEMBLAGES
MISE en POT des ASSEMBLAGES en cas de RUPTURE de GAINE
STOCKAGE Na
REACTEUR 1000 MWé
SECTION du BATIMENT PILE
COUPE : cf Fig VI. 12
ECHELLE :

FIGURE: VI.14

CHAPITRE VII

ETUDE DU COMPORTEMENT DYNAMIQUE DU REACTEUR DE REFERENCE (1000 MWe)

I - INTRODUCTION

On sait que, parmi les problèmes nouveaux posés par le développement des réacteurs rapides, l'étude de leur comportement dynamique, c'est-à-dire de leur stabilité dans toutes les configurations envisageables et de leur évolution consécutive à des perturbations même très improbables, est d'une grande importance pour l'appréciation de leur sûreté.

Il a été en effet montré [11] et [12] que les réacteurs rapides de grands volumes pouvaient avoir des coefficients de réactivité dus au sodium assez fortement positifs au centre du réacteur, mais que par contre on pouvait compter sur un coefficient Doppler relativement important et négatif dans tout le réacteur.

Nous allons montrer dans cette étude l'influence de ces coefficients sur la stabilité et les régimes transitoires du réacteur défini dans le chapitre précédent, en nous basant sur des valeurs calculées des coefficients de réactivité, puis en procédant à une étude paramétrique simplifiée permettant de dégager les tendances de la philosophie du contrôle des réacteurs de ce type.

II - COEFFICIENTS DE REACTIVITE

1°, Coefficients de danger

Les coefficients de danger ont été calculés avec le découpage de la figure VII-1 par un code de perturbation.

Il subsiste certaines incertitudes sur l'effet Doppler et sur le coefficient sodium ; on peut penser cependant que la répartition spatiale reste valable. Nous nous sommes attachés, dans ce qui suit, à évaluer les conséquences de variations éventuelles des valeurs de ces coefficients.

Les figures VII-2 à 11 montrent la répartition des coefficients de danger des principaux constituants et de l'effet Doppler. Pour celui-ci, nous avons tenu compte d'une loi de variation en $T^{-3/2}$, hypothèse réaliste pour les hautes températures. Les coefficients sodium et acier sont positifs au centre du coeur et négatifs à la périphérie, le coefficient combustible est négatif dans tout le coeur ainsi que le coefficient Doppler.

Le remplacement d'un assemblage :

- de la zone coeur intérieure par un assemblage de la zone coeur extérieure, donne une réactivité de 56 pcm (1 pcm = 10^{-5} $\frac{\Delta k}{k}$)
- de la couverture radiale par un assemblage de la zone coeur extérieure, donne une réactivité de 37 pcm.

2°, Coefficients de réactivité isothermes

Les coefficients isothermes sont donnés dans le tableau VII-1. Les deux principales hypothèses faites sont :

- le combustible est lié à la gaine,
- les assemblages sont munis de plaquettes aux 3/5 du coeur et le coeur est rigide lorsque le gradient nominal de température est atteint dans le coeur.

On peut remarquer que :

- les deux effets prépondérants sont le coefficient Doppler et les coefficients dus aux structures.
  Ces coefficients sont négatifs.

- les différents coefficients liés aux dilatations, à l'exception des coefficients dus aux structures, se compensant approximativement.
- il semble donc que, même dans l'hypothèse pessimiste où les coefficients Doppler et structures auraient été surestimés d'un facteur important (3 par exemple), le coefficient isotherme total serait néanmoins largement négatif.
- le coefficient dû à la déformation des assemblages (bowing) après compactage du coeur, est négligeable.

3°, Coefficients de puissance

Les coefficients de puissance sont donnés dans le tableau VII-2. La contribution de l'effet Doppler au coefficient de puissance est prépondérante aussi bien à débit nominal qu'à faible débit[13]. Il faudrait diviser le coefficient Doppler par 3,7 et multiplier le coefficient sodium par la même valeur 3,7 pour annuler le coefficient de puissance au débit dixième du débit nominal. On peut donc estimer que le coefficient de puissance restera négatif malgré les incertitudes sur les coefficients de réactivité.

4°, Réserve de réactivité

La réserve de réactivité doit compenser l'antiréactivité due :

- au coefficient isotherme pour passer de 150° à 400° à l'entrée du réacteur (cela suppose que l'installation est préchauffée à l'aide de la puissance nucléaire) : 1,4 $

13) Nous avons arbitrairement pris dans ce cas, un débit 1/10 du débit nominal, hypothèse probablement pessimiste étant donné que les procédures d'exploitation élimineront le fonctionnement à débit aussi faible.

$$\psi_I^+(\tau_1) = \psi_I^-(\tau_1) = \psi_I(\tau_1)$$

$$\psi_X^+(\tau_1) = \psi_X^-(\tau_1) = \psi_X(\tau_1) \qquad (14)$$

Because of the fact that the Hamiltonian is zero for two different values of P , we can define a set of two equations and two unknowns : $\psi_I(\tau_1)$ and $\psi_X(\tau_1)$.

$$\Omega_i \Sigma_f \psi_I(\tau_1) + (\Omega_x \Sigma_f - \sigma_x X_m)\, \psi_X(\tau_1) = 0$$

$$\psi_o - \lambda_1 I(\tau_1)\, \psi_I(\tau_1) + (\lambda_i I(\tau_1) - \lambda_x X_m)\, \psi_x(\tau_1) = 0$$

Consequently, the adjoined variables for the pair of adjoining sections are completely determined as far as the junction point is known.

Computer results, show that the section in the interior of G does not contain switching points. Consequently, it must go through the initial point (I_o , X_o) and therefore it becomes the first section of the optimal trajectory. At the same time the junction point $(I(\tau_1), X_m)$ is determined.

b). The trajectory leaves the boundary X_m of G with a control $P_{op}(t) = P_{max}$, if at the junction time τ_2 we have $P_c(\tau_2) > P_{min}$. Consequently,

$$H(\psi_I^+ , \psi_X^+ , I, X_m , P_{max}) = 0 \qquad (15)$$

$$\psi_I^+(\tau_2) = \psi_I^-(\tau_2) = \psi_I(\tau_2)$$

$$\psi_X^+(\tau_2) = \psi_X^-(\tau_2) + \mu \qquad (16)$$

(μ is a real number)

For every point $(I(\tau_2), X_m)$ we can find a value of μ satisfying (15). This completely determines the trajectory in the interior of G. It does not contain switching points (to be tested numerically) and consequently it goes necessarily through the final point (I_1, X_1).

c). The trajectory can also leave the boundary X_m of G because $P_c(t)$ has reached the value P_{min}. This immediately fixes $(I(\tau_2), X_m)$. The conditions (16) are still valid, but

$$H(\psi_I^+, \psi_X^+, I, X_m, P_{min}) = 0 \qquad (17)$$

is automatically satisfied for every value of μ. This degree of liberty gives us the possibility of determining a switching point in the interior of G making the trajectory go through its final point (I_1, X_1) .

4. Discussion of the Optimal Solution

Although Pontryagin's theorems only offer necessary conditions for optimality, we should not forget that they form a complete set of conditions. This means that by numerical verifications with the computer - we have already referred to them several times in §3 - we can be practically sure of the existence and uniqueness of the optimal solution (*).

Once the numerical verificationsare made we do not need anymore the adjoined variables, jump conditions, etc. in order to proceed to the synthesis of the final solution. With the curves of figures 1 and 2 it can be done almost graphically.

Let us consider some cases of particular interest.

Case 1 : $P_{min} << P_1 << P_o < P_{max}$

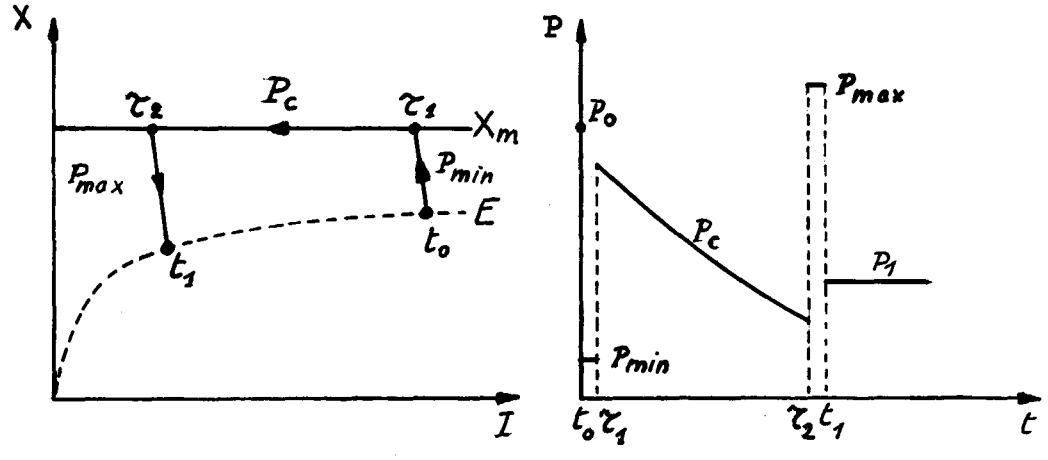

fig. 3

(*) Remember that the existence theorems asking for the convexity of $f(x, U)$ (see e.g. ref. [9]) already guarantee the existence of the sections separately. An effort to include the junction conditions as well would be of interest in the theory of optimal control.

A typical result calculated for an ORGEL-type reactor is:

P_o = 618 kcal/s
P_1 = 200 kcal/s
P_{min} = 0 kcal/s
P_{max} = 1000 kcal/s
ρ_{xs} = 20‰ (X_m=1,66 X_o)

$\tau_1 - t_o$ = 0.4 h
$\tau_2 - \tau_1$ = 24.0 h
$t_1 - \tau_2$ = 0.2 h
$t_1 - t_o$ = 24.6 h

Case 2 : $P_{min} \lesssim P_1 \ll P_o < P_{max}$

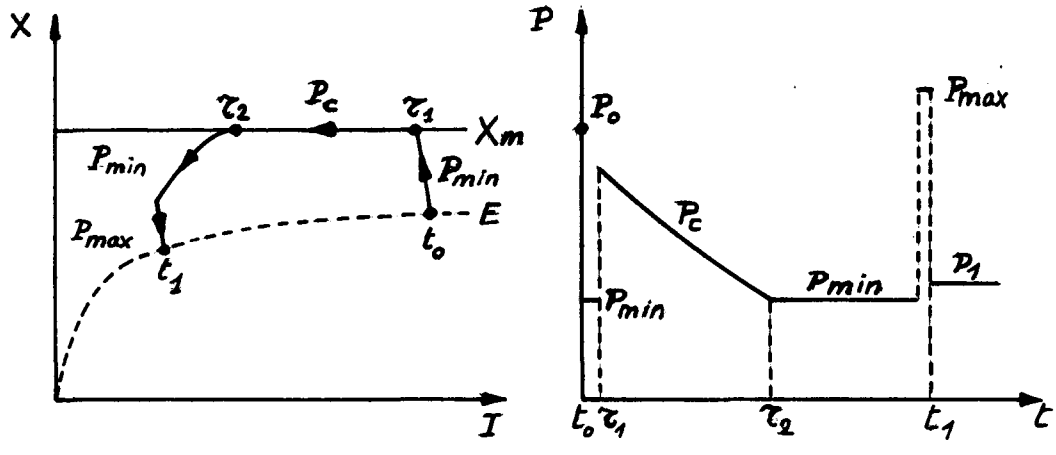

fig. 4

Notice that for $P_{min} = P_1$, although a very realistic assumption, the minimum time $t_1 - t_o$ becomes infinite ! Evidently, the corresponding trajectory should be considered only as a limiting case of the optimal solutions for $P_{min} \to P_1$. We shall come back to this point later on.

Case 3 : $P_{min} < P_1 \tilde{\sim} P_o < P_{max}$

This case where the constraint X_m is not reached at all is less interesting. The optimal control contains a switching point of the type (P_{max}, P_{min}) .

5. The Influence of the Parameters P_{max} and P_{min} .

Typical for case 1 are the small values of $\tau_1 - t_o$ and $t_1 - \tau_2$. For this reason the transition time $t_1 - t_o$ is not sensitive to variations of P_{max} and P_{min} (on condition that $P_{min} << P_1$). The particular but realistic case $P_{max} = P_o$ does not imply a particularly unfavourable result.

On the contrary, the "insensitivity" of P_{max} can be exploited. The third section being uninteresting from the energy point of view, it would be reasonable to accept a new optimization criterion

$$\frac{dx^{\circledast}}{dt} = 1 + a\,(P)^2 \tag{18}$$

The equations are only slightly modified, except that, between the values P_{min} and P_{max} , P(t) may vary continuously

$$P_{op}(t) = - \frac{\left[\Omega_i \Sigma_f \psi_I(t) + (\Omega_x \Sigma_f - \sigma_x X)\psi_X(t)\right] K}{2a\,\psi_o} \tag{19}$$

For this law we ought to know the numerical values of $\psi_I(t)$ and $\psi_X(t)$, and this seriously complicates the calculations. Figures 1 and 2 are no longer sufficient for the synthesis.

As far as parameter "a" (see (18)) is concerned, it can be chosen such that a good compromise between minimum time and excessive loss of energy is assured.

All these considerations justifie a posteriori the exclusion from our model of all phenomena (reactor kinetics equations e.g.) incompatible with an instantaneous variation of $P(t)$. Otherwise, the mathematical and numerical analysis would have been considerably complicated without significant improvement of the result.

From an examination of figure 4 it is clearly apparent why the transition time $t_1 - t_o$ grows rapidly when P_{min} and P_1 tend to each other. In order to remedy this disadvantage we shall propose modified final conditions for (I_1 , X_1) (see §7).

6. Influence of Parameter ρ_{xs} (or X_m)

The minimum time $t_1 - t_o$ is represented in figure 5 as a function of ρ_{xs}. We have compared it with another function $\theta(\rho_{xs})$, which is defined as follows:

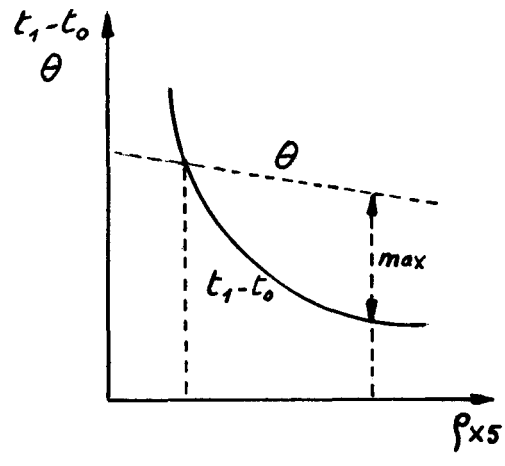

fig. 5

Imposing an instantaneous shut-down of the reactor at time t_o, the xenon concentration would rise rapidly - passing the level X_m and attaining a maximum - and then would go down, becoming smaller than X_m at the time θ after t_o, called the recovery time. At that instant the reactor can be started again and brought to the power level P_1. This type of control is perhaps not realistic, but it makes a useful comparison with our optimal solutions possible. It appears, for instance, that $\theta < t_1 - t_o$ for $\rho_{xs} < 7‰$ (ORGEL-type reactor), which should not be surprising. We also find a maximum value for $\theta - (t_1 - t_o)$ for $\rho_{xs} \cong 26‰$.

7. Influence of the Final Conditions

Other than for facilitating computation, there is no reason to require that the points (I_o, X_o) and (I_1, X_1) be equilibrium points for the reactor.

Moreover, for initial points $(I_o, X_o) \notin E$, nothing prevents us from using the previously obtained results in the same way for the synthesis of the optimal control.

However, for the final points (I_1, X_1) this is no longer true. On one hand, if $(I_1, X_1) \in E$ we risk too long control periods (see case 2). On the other hand, if $(I_1, X_1) \notin E$ we must take care that the xenon never exceeds the value X_m in the post-control period $(t > t_1)$.

Let us agree on a new formulation of our problem, the final conditions being defined as follows:

The new point (I_1', X_1') is not given, but should belong to the set B, which is defined by the curve $\varphi(I, X) = 0$. This curve is a solution of system (1) for $P(t) = P_1$ and it is tangent to the constraint $X = X_m$ (see fig. 6).

Let us call $t_1' - t_o$ the minimum transition time for this problem.

The adjoint vector $(\psi_I(t_1')\ ,\ \psi_X(t_1'))$ must now be perpendicular to $\varphi(I, X) = 0$ (transversality conditions).

$$\frac{\psi_I(t_1')}{\psi_X(t_1')} = \frac{\partial\varphi/\partial I}{\partial\varphi/\partial X}_{(\varphi=0)} \qquad (20)$$

These conditions cannot be verified without computing $(\psi_I(t), \psi_X(t))$ along the whole trajectory. For this reason we cannot do without the computer for the synthesis of the optimal control. Indeed, a graphical construction with figures 1 and 2 becomes impossible.

Fortunately, we can approximate (I_1', X_1') with other final conditions which are easier to test with graphical means. It can be done as follows.

In figure 6 we have constructed the set of points which can be attained in a time $t_1' - t_o$ by a minimum time trajectory starting from (I_o, X_o). We know from the theory (see e.g. ref. [6]) that wherever this set has a normal, this normal coincides with the adjoint vector $[\psi_I(t_1'), \psi_X(t_1')]$, which itself has to be normal to B (20). This immediately fixes the point (I_1', X_1'). For numerical reasons it also appears that :

1° (I_1', X_1') lies slightly above E(*).

2° the point $(I_1'', X_1'') = E \cap B$ is attainable in a time $t_1'' - t_o$ which is only slightly larger than $t_1' - t_o$.

(*) Note that the angle at which the trajectories $P(t) = c^t$ cut the set E at a given point does not depend on P.

Accepting the approximation of (I_1', X_1') with $(I_1'', X_1'') \in E$, we have again a problem of the type of §2, which can be solved by graphical construction.

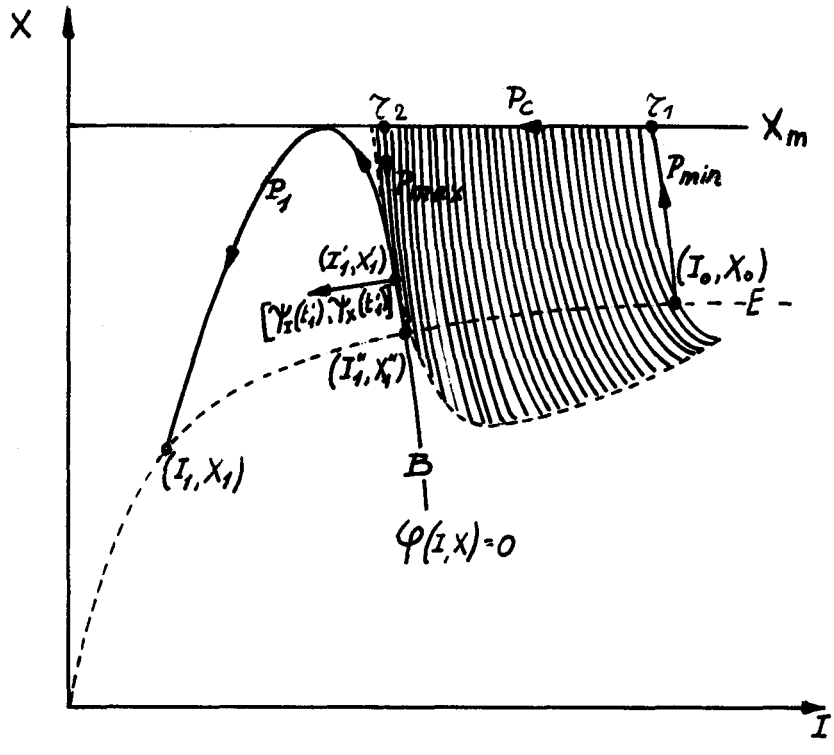

fig. 6

A typical result corresponding to the data of case 1 (§4) is :

$$\tau_1 - t_o = 0.4 \text{ h}$$
$$\tau_2 - \tau_1 = 8.8 \text{ h}$$
$$t_1'' - \tau_2 = 0.3 \text{ h}$$
$$t_1'' - t_o = 9.5 \text{ h}$$

Obviously $t_1'' - t_o \ll t_1 - t_o$. Moreover, the disadvantages of case 2 (§4) are eliminated and the parameter P_{min} has becomeas insensitive as P_{max} (§5). On the other hand, equilibrium is attained only after an infinite time.

8. Minimum Xenon Buildup

The version of the xenon problem , which is usually found in literature (see ref. [2] , [3] , [4] , [5]) only considers the shut-down of the reactor. It can be formulated as follows.

It is required to shut the reactor down to zero power in an allowable time "b". Following time b, however, xenon concentration X(t) will rise to a maximum X_{max} . We should find the optimal shut-down program minimizing $X_{max}[P(t)] = J(P)$. For slightly different optimization criteria, see ref.[5].

We do not want to comment on the opportuneness of this formulation. Yet, as has been stated already in ref. [4] , the optimal solution becomes again a minimum time one. Finally, it appears that the key of the xenon problem is not so much the choice of the optimization criterion, but the right manipulation of the state constraints (to be compared with ref. [3]). Note also, that, if b is so small that the state constraint X_m can be ignored (which is assumed implicitely in ref. [2]), the criterion J(P) is so flat in the neighbourhood of the optimum, that it does not matter how the reactor is shut down (indeed, "The sport is not worth the candle"! ref. [2] , p. 152).

9. The Method of Penalty Functions

This method (see ref. [8], ch.3) apparently avoids the state constraint difficulties, introducing them directly in the optimization criterion by penalty functions.

In this case the new function $f^{0*}(x, u)$ is given by

$$f^{0*}(I, X, P) = 1 + k_p \left(\frac{dX}{dt}\right)^2 \qquad (21)$$

The positive constant $k_p = 0$ for $X < X_m$

k_p = large for $X \geq X_m$

Following the techniques developed in ref. [7] the optimal solution can be obtained directly by the computer. For growing values of k_p one can construct a series of optimal trajectories (see fig. 7) converging to the solution of the original problem.

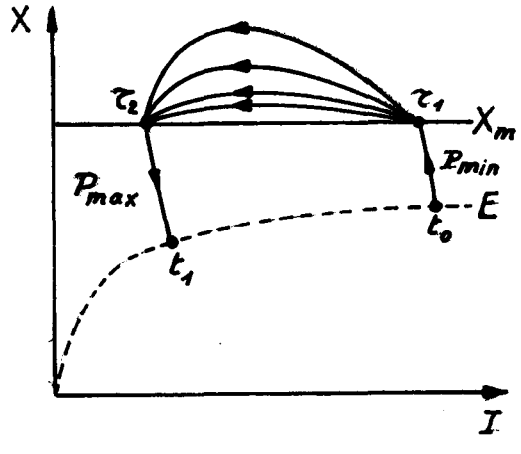

fig. 7

The method is definitely more elegant and more general than the sequence of particular developments presented in §3. Unfortunately, the programming difficulties are considerable and the accuracy, at least in our case, is very bad. Indeed, the trajectories are too sensitive to variations of $(\psi_I(t_o), \psi_X(t_o))$ to allow the final conditions (I_1, X_1) to be reasonably satisfied. Going back to the arguments of §3.3.a it is easy to understand why.

On the other hand, with a direct explication of the Gamkrelidze conditions, we have obtained accurate results and developed a practical technique in two steps:

- Calculation of the family of curves of figures 1 and 2,
- Final synthesis by graphical construction.

10. The Optimal Controller

Until now we have found an optimal program $P_{op}(t)$ but not a real synthesis of an optimal controller $P_{op}(I, X)$ in its narrow sense. If mathematically one can be deduced from the other, the practical implementation of $P_{op}(I, X)$ puts new supplementary problems concerning the observability of the variables I and X.

Measuring the period of the reactor, X(t) could be deduced indirectly from the motion of the control rods, but for I(t) the difficulties are greater. It may be necessary to include at least a part of model (1) into the controller, where it is functionning in parallel with the physical system. This again puts the question of the validity of the model and the sensitivity of the physical parameters. It might very well happen that after a study of these difficulties the formulation of the xenon problem should be changed once more.

Acknowledgements

The author is indebted to Mr. Palinski for his contributions to the formulation of the problem, especially for the physical aspects and the numerical data, and to Mrs. M. Gutmann for programming the equations.

References

[1] L.S. Pontryagin, V.G. Boltyanskii, R.V. Gamkrelidze, E.F. Mishchenko, The Mathematical Theory of Optimal Processes, John Wiley & Sons, New York, 1962.

[2] M. Ash, R. Bellman, R. Kalaba, On Control of Reactor Shut-down Involving Minimal Xenon Poisoning, Nuclear Science and Engineering, Vol.6, pp. 152-156, 1959.

[3] Z.R. Rosztoczy, L.E. Weaver, Optimum Reactor Shutdown Program for Minimum Xenon Buildup, Nuclear Science and Engineering, Vol.20, pp. 318-323, 1964.

[4] Y. Shinohara, J.Valat, Optimalisation de l'empoisonnement par minimilisation du pic xénon, C.R. Acad. Sc. Paris, t. 259, 31 août 1964, pp. 1623-1626.

[5] Y. Shinohara, J. Valat, Optimalisation de l'empoisonnement par optimalisation de l'incubation ou de la guérison, C.R. Acad. Sc. Paris, t. 259 14 septembre 1964, pp. 1836-1839.

[6] H. Halkin, The Principle of Optimal Evolution, Proc. 2nd Int. Symp. on Nonlinear Mechanics and Nonlinear Differential Equations, Academic Press, New York, 1962.

[7] W. De Backer, Synthesis of Optimal Control and Hybrid Computation, 4th Int. Analogue Computation Meeting, Brighton, United Kingdom - Sept. 14-18, 1964. - EURATOM report EUR 2202 e.

[8] W. De Backer, The Maximum Principle, its Computational Aspects and its Relations to other Optimization Techniques, EURATOM report, EUR 590 e.

[9] F. Roxin, The Existence of Optimal Controls, Michigan Mathematical Journal, vol.9, pp.109-119, 1962.

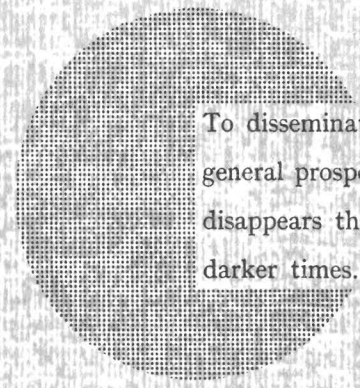

To disseminate knowledge is to disseminate prosperity — I mean general prosperity and not individual riches — and with prosperity disappears the greater part of the evil which is our heritage from darker times.

Alfred Nobel

EURATOM – C.I.D.
51 - 53, rue Belliard
Bruxelles (Belgique)